SDC-91-00009

DI
T

SDC
SOLENOIDAL DETECTOR NOTES

LEPTONIC ASYMMETRIES ASSOCIATED WITH A Z'

G. Eppley, H. E. Miettinin

March 1991

March, 1991 SDC-91-00009

LEPTONIC ASYMMETRIES ASSOCIATED WITH A Z'

G. Eppley and H.E. Miettinen

T.W. Bonner Nuclear Laboratory, Physics Department, Rice University
Houston, TX 77251-1892

Abstract

We discuss the measurement of leptonic asymmetries, A_{fb}, associated with a Z' of mass 1–4 TeV. The dependence of A_{fb} on both the dilepton rapidity and the dilepton mass is examined in some detail. Three distinct models for the Z' are considered. We find that the measurement of off-peak asymmetries is likely to be of only limited value due to a combination of low statistics, acceptance limitations at small angles, and a large asymmetry inherent in the standard model. The measurement of on-peak asymmetries would not benefit significantly from extension of lepton pseudorapidity coverage beyond $|\eta| = 2.5$.

1. Introduction

The detection of a heavy Z' at the SSC has been discussed in many previous studies, both in general terms [1] and in the context of the SDC detector [2]. Using the mode $Z' \to e^+e^-$, the mass of a few TeV Z' should be measurable to a precision of about 0.1% in a few years. The total width, expected to be in the range 10–200 GeV, could be measured to an accuracy better than 10% in a favorable case. There should be no significant competing backgrounds to $Z' \to e^+e^-$ or $Z' \to \mu^+\mu^-$.

The understanding of the nature of a Z' is largely a question of measuring the total width, Γ, the leptonic branching ratio, B, and the leptonic forward-backward asymmetry A_{fb}. The asymmetry arises because of the parity violating production and decay of the Z', coupled with the fact that the x distributions of quarks and antiquarks in the initial protons are quite different. (For example, for a Z' with standard model couplings to quarks and leptons, a fast, forward Z' is likely to have arisen from an annihilation of a large x quark and a small x antiquark, resulting in a negative helicity Z'. The subsequent decay $Z' \to e^+e^-$ prefers an orientation where the electron is emitted in the same direction as the Z' in the CM frame). A_{fb} increases with the rapidity of the Z', and it also depends on the mass of the lepton pair because the interference effects between the Z' and the γ^*/Z background become relatively more important off the resonance peak.

In this study we have addressed two questions:

a) Does the measurement of off-peak asymmetries yield important additional information about the Z' couplings, beyond what can be learned from the measurements of total width, Γ, leptonic branching ratio, B, and on-peak asymmetries?

b) Would the measurement of on-peak asymmetries benefit from an extended pseudorapidity coverage of the SDC detector beyond $|\eta| = 2.5$, given that A_{fb} increases with rapidity, y?

We have used the Lund Monte Carlo program Pythia (version 5.4) in our study. The matrix elements in Pythia invoke the full $\gamma^*/Z/Z'$ structure with interference. The SDC detector parameters are taken from Ref. 3. Only the e^+e^- final state is considered here since the mass resolution for electron pairs is in general considerably better than that for muon pairs.

We find that the answer to both questions posed above appears to be no.

2. Asymmetry in the Standard Model

The leptonic asymmetry A_{fb} is defined as:

$$A_{fb} = \frac{\sigma(\theta < \pi/2) - \sigma(\theta > \pi/2)}{\sigma(\theta < \pi/2) + \sigma(\theta > \pi/2)}$$

where θ is the angle between the dilepton momentum in the CM frame and the momentum of the negatively charged lepton in the dilepton rest frame. A_{fb} is an even function of the rapidity, y, of the $\gamma^*/Z/Z'$. Fig. 1 shows A_{fb} in the standard model as a function of $|y|$ for low mass ($M \simeq 200$ GeV) and high mass ($M \simeq 2$ TeV) lepton pairs. In both cases A_{fb} increases with y, but at quite different rates: for low mass pairs A_{fb} is substantial only in the intermediate and forward regions whereas for high mass pairs A_{fb} increases rapidly with y since a very large x quark is required to give the lepton pair both mass and longitudinal momentum.

In the following we limit ourselves to the region $|y| > 0.3$ since A_{fb} is small in the very central region. Figs. 2a and 2b show A_{fb} in the standard model as a function of the dilepton mass. Fig. 2a shows A_{fb} in the vicinity of the Z, and Fig. 2b shows A_{fb} for larger dilepton masses up to 4 TeV. Two features of A_{fb} are worth emphasizing. First, in the vicinity of the Z there is a prominent dip structure due to γ^*/Z interference. The minimum in A_{fb} occurs near 70 GeV, where the cross-section due to the tail of the Z is comparable to that of the Drell-Yan background. As we will see later, similar structure is associated with the Z''s we have studied. Second, at large dilepton masses the asymmetry is quite large, in the 30–40% range, and increasing slowly with $M_{l^+l^-}$.

At the Z mass, the asymmetry is very small. We find a value $A_{fb} = 0.024 \pm 0.004$ integrated over the range $M_Z \pm \Gamma_Z$. For comparison, the CDF collaboration has measured a value $A_{fb} = 0.052 \pm 0.059 \pm 0.004$ in $\bar{p}p$ collisions at $\sqrt{s} = 1.8$ TeV [4].

We have verified that the structure in the vicinity of the Z is unaffected by the presence of a (narrow) Z' of mass 1 TeV or above. Only an unnaturally wide Z' could have an effect near the Z mass.

3. Acceptance effects

The "generic" SDC detector will identify and measure leptons in the range $|\eta| < 2.5$. This limitation is particularly severe for the measurement of low mass lepton pairs. Fig. 3 shows the dilepton mass versus the rapidity of the lepton pair. Simple

kinematics dictates that the width of the rapidity distribution narrows significantly with increasing dilepton mass. Fig. 4 shows the acceptance for dileptons of mass M as a function of the maximum lepton pseudorapidity coverage, ηmax (i.e. both leptons must have $|\eta| < \eta$max). It is clear that most low mass lepton pairs can not be measured with high efficiency in a realistic detector. Thus potentially large asymmetries, arising from large rapidities regardless of the model, are substantially diluted by the detector acceptance especially for low mass ($<$ 500 GeV) lepton pairs. This is shown explicitly in Fig. 5, where we plot the theoretical asymmetry curves of Fig. 2 together with the corresponding "measured" curves for $|\eta| = 2.5$. The errors in the "data" of Fig. 5 reflect the statistical accuracy to be expected in one SSC year (an integrated luminosity of $10^4/pb$). The prominent structure in the vicinity of the Z is all but washed out by poor acceptance at forward angles. In the TeV region, on the other hand, large theoretical asymmetries are easily detected, given sufficient statistics.

4. Asymmetries for the Z'

We now introduce a Z' of mass 1–4 TeV into the picture. Three distinct models for the Z' couplings are considered:

a) A Z' with standard model couplings to quarks and leptons ("heavy Z" model).

b) A conventional left-right symmetric model (LR) of Ref. 5. In addition to a Z', this model contains a new, heavy right-handed W'.

c) An alternative left-right symmetric model (ALR) of Ref. 6. This model allows for a light ($\approx$ 300 GeV) right-handed W' with unusual properties (e.g. non-zero lepton number).

Table 1 shows the width of a 1 TeV Z' in the three models. The width of a Z' is expected to scale as its mass. Also shown in Table 1 are the numbers of events produced in the interval $M_{Z'} \pm \Gamma_{Z'}$ in one SSC year. The Z' production cross-section falls with increasing mass approximately as $1/M_{Z'}^4$.

Figs. 6–8 show the asymmetry A_{fb} in the three models for a 1 TeV Z' as a function of the dilepton mass. The standard model asymmetry curve is superimposed on each figure. Several points are of interest:

i) In all three cases A_{fb} deviates very significantly from the standard model asym-

metry in the immediate vicinity of the Z'. Off the resonance peak this deviation may be further enhanced by interference effects between the Z' and the γ^*/Z amplitudes in the mass region below the Z' where the two amplitudes have comparable magnitudes. This is the case in the "heavy Z" model in particular.

ii) The width of the observed structure in A_{fb} is roughly proportional to $\Gamma_{Z'}$. The effect of the Z' is "felt" over a rather large range in $M_{l^+l^-}$: in the "heavy Z" model this range extends from ≈ 500 GeV to ≈ 1300 GeV. This makes it possible to study , in principle, the nature of a Z' by making use of dileptons whose mass is well below the resonance peak, and which therefore have a production cross-section much higher than those adjacent to the peak.

iii) The tails of the asymmetry curves in the three models coincide with the standard model background on the low mass side since A_{fb} is then determined entirely by γ^*/Z interference. On the high mass side A_{fb} is determined by the interference of the Z' with the standard model background, and it then obviously depends on the nature of the Z'.

From these figures it is clear that extracting useful new information from the measurement of off-peak asymmetries is going to be difficult. Near the resonance peak event rates are of course extremely low. In the mass range well below the peak event rates are higher, and the asymmetry is quite large, but the large value of A_{fb} merely reflects known physics in the standard model and does not bear upon the nature of the Z'. One must also keep in mind that limited acceptance for low mass lepton pairs dilutes the theoretical asymmetry. As an example, Fig. 9 shows the "measured" A_{fb} in the "heavy Z" model, along with the theoretical curve and the standard model curve. The errors are for one SSC year. Similar results are obtained for the two other models.

Finally we note that in the mass region well above the Z mass, A_{fb} exhibits scaling behavior, i.e. A_{fb} depends only on the ratio $M_{l^+l^-}/M_{Z'}$, and not on the two masses separately (see Fig. 10). This is a direct consequence of the fact that $\Gamma_{Z'}$ is proportional to $M_{Z'}$. Thus our discussion above applies equally well to any Z', regardless of its mass. For low mass lepton pairs scaling does not hold, of course, since M_Z becomes a relevant variable.

5. Detector implications

What about on-peak asymmetry measurements? Would something be gained by increasing the rapidity coverage for leptons beyond $|\eta| = 2.5$? The answer is not really, since the acceptance for a Z' of mass $M > 1$ TeV is already quite good. The present lower limit on the Z' mass, assuming standard model couplings, is 380 GeV [7]. Table 2 gives the "measured" A_{fb} and its error for a 1 TeV Z' in the three models for $\eta\,\mathrm{max} = 2.5$ and $\eta\,\mathrm{max} = 3.0$. The errors correspond to one SSC year and A_{fb} is integrated over the mass range $M_{Z'} \pm \Gamma_{Z'}$. There is little advantage in increasing the forward acceptance for leptons. For a heavier Z' the gain is even smaller.

6. Summary

We have studied the utility of leptonic asymmetry measurements associated with a Z' of mass 1–4 TeV. We conclude that the planned pseudorapidity coverage of the SDC detector for leptons, $|\eta| < 2.5$, is sufficient for a good measurement of on-peak asymmetries. Off-peak asymmetry measurements, of course, suffer from low statistics. An exception is the mass region well below the resonance peak, but then the asymmetry, A_{fb} (in the three models we have studied), is only marginally different from that in the standard model. Poor acceptance for low mass lepton pairs makes it even harder to distinguish among models. We conclude that off-peak asymmetry measurements may not be terribly helpful, mostly because the rates are reasonable only in the low mass region where the physics is not of overwhelming interest.

We thank Paul Stevenson for helpful conversations. This work was supported in part by U.S. Department of Energy Contract DE–AS05–76ERO5096.

References

[1] V. Barger, N.G. Deshpande, J.L. Rosner, and K. Whisnant, Phys. Rev. D **35**, 2893 (1987).
J.L. Rosner, Phys. Rev. D **35**, 2244 (1987).

[2] I. Hinchliffe, M. Shapiro, and M. Mangano, SDC-90-00036.
I. Hinchliffe and M.D. Shapiro, SDC-90-00115.
G. Eppley and H.E. Miettinen, SDC-90-00125.

[3] I. Hinchliffe, SDC-90-00100.

[4] L.G. Pondrom, in *Proceedings of the Twenty-Fifth International Conference on High Energy Physics, Singapore, August, 1990*, (Fermilab preprint FERMILAB-Conf-90/256-E).

[5] For a general survey, including original references, see R.N. Mohapatra, *Unification and Supersymmetry*, Springer-Verlag, New York, 1986. For a discussion in the context of the SSC, see J.A. Grifols, A. Mendez, and R.M. Barnett, Phys. Rev. D **40**, 3613 (1989).

[6] E. Ma, Phys. Rev. D **36**, 274 (1987); Mod. Phys. Lett. A **3**, 319 (1988).
V. Barger and K. Whisnant, Int. J. Mod. Phys. A **3**, 879 (1988).

[7] CDF Collaboration, presented by J. Skarha, Fermilab preprint FERMILAB-Conf-90/242-E (1990).

TABLE CAPTIONS

Table 1. The width, Γ, and the number of events produced in the interval $M_{Z'} \pm \Gamma_{Z'}$ in one SSC year for each of the three models studied.

Table 2. A_{fb} integrated over the interval $M_{Z'} \pm \Gamma_{Z'}$ for a 1 TeV Z' in the three models studied. The first column corresponds to perfect acceptance, the second column to $\eta\,\mathrm{max} = 2.5$, and the third column to $\eta\,\mathrm{max} = 3.0$. The errors are for one SSC year.

FIGURE CAPTIONS

Fig. 1. A_{fb} versus $|y|$ in the standard model for low mass ($M_{e^+e^-} \simeq 200$ GeV) and high mass ($M_{e^+e^-} \simeq 2$ TeV) lepton pairs.

Fig. 2. a) A_{fb} versus $M_{e^+e^-}$ in the standard model for $20 < M_{e^+e^-} < 200$ GeV.
b) A_{fb} versus $M_{e^+e^-}$ in the standard model for $M_{e^+e^-} < 4$ TeV.

Fig. 3. Dilepton mass versus the rapidity of the lepton pair. The events were generated such that the number of events per unit $\log M$ is constant.

Fig. 4. The acceptance for lepton pairs versus ηmax. Both leptons are required to have $|\eta| < \eta$max. $M_{e^+e^-}$ varies from M_Z (lowest curve) to 4 TeV (highest curve).

Fig. 5. a) The effect of acceptance on the measurement of A_{fb} versus $M_{e^+e^-}$ for $20 < M_{e^+e^-} < 200$ GeV. The solid curve represents the standard model A_{fb} from Fig. 2a. The error bars correspond to one SSC year.
b) Same as a) except for $M_{e^+e^-} < 4$ TeV.

Fig. 6. A_{fb} versus $M_{e^+e^-}$ for a 1 TeV Z' with standard model couplings. The solid curve is the standard model A_{fb} from Fig. 2b.

Fig. 7. Same as Fig. 6 except with LR couplings.

Fig. 8. Same as Fig. 6 except with ALR couplings.

Fig. 9. The effect of acceptance on the measurement of A_{fb} versus $M_{e^+e^-}$ for a 1 TeV Z' with standard model couplings. The heavy solid curve is the standard model A_{fb} from Fig. 2b. The lighter curve is the predicted A_{fb} for a 1 TeV Z' from Fig. 6. The error bars correspond to one SSC year.

Fig. 10. A_{fb} versus $M_{e^+e^-}/M_{Z'}$ for a 1, 2, and 4 TeV Z' with standard model couplings. A_{fb} exhibits scaling behavior.

Table 1

$Z'/Z/\gamma^* \to e^+e^-$ $M_{Z'} = 1$ TeV

Model	$\Gamma_{Z'}$(GeV)	Number of events in $M_{Z'} \pm \Gamma_{Z'}$ in one SSC year
Standard model couplings	31.0	22.6×10^3
LR	11.9	8.3×10^3
ALR	8.3	15.1×10^3

Table 2

$Z'/Z/\gamma^* \to e^+e^-$ $M_{Z'} = 1$ TeV

Model	A_{fb} perfect acceptance	A_{fb} η max = 2.5	A_{fb} η max = 3.0
Standard model couplings	.044	$.030 \pm .010$	$.036 \pm .009$
LR	.095	$.056 \pm .017$	$.072 \pm .015$
ALR	$-.21$	$-.14 \pm .01$	$-.17 \pm .01$

Table 1

$Z'/Z/\gamma^* \to e^+e^-$ $M_{Z'} = 1$ TeV

Model	$\Gamma_{Z'}$(GeV)	Number of events in $M_{Z'} \pm \Gamma_{Z'}$ in one SSC year
Standard model couplings	31.0	22.6×10^3
LR	11.9	8.3×10^3
ALR	8.3	15.1×10^3

Table 2

$Z'/Z/\gamma^* \to e^+e^-$ $M_{Z'} = 1$ TeV

Model	A_{fb} perfect acceptance	A_{fb} η max = 2.5	A_{fb} η max = 3.0
Standard model couplings	.044	$.030 \pm .010$	$.036 \pm .009$
LR	.095	$.056 \pm .017$	$.072 \pm .015$
ALR	$-.21$	$-.14 \pm .01$	$-.17 \pm .01$

Figure 1

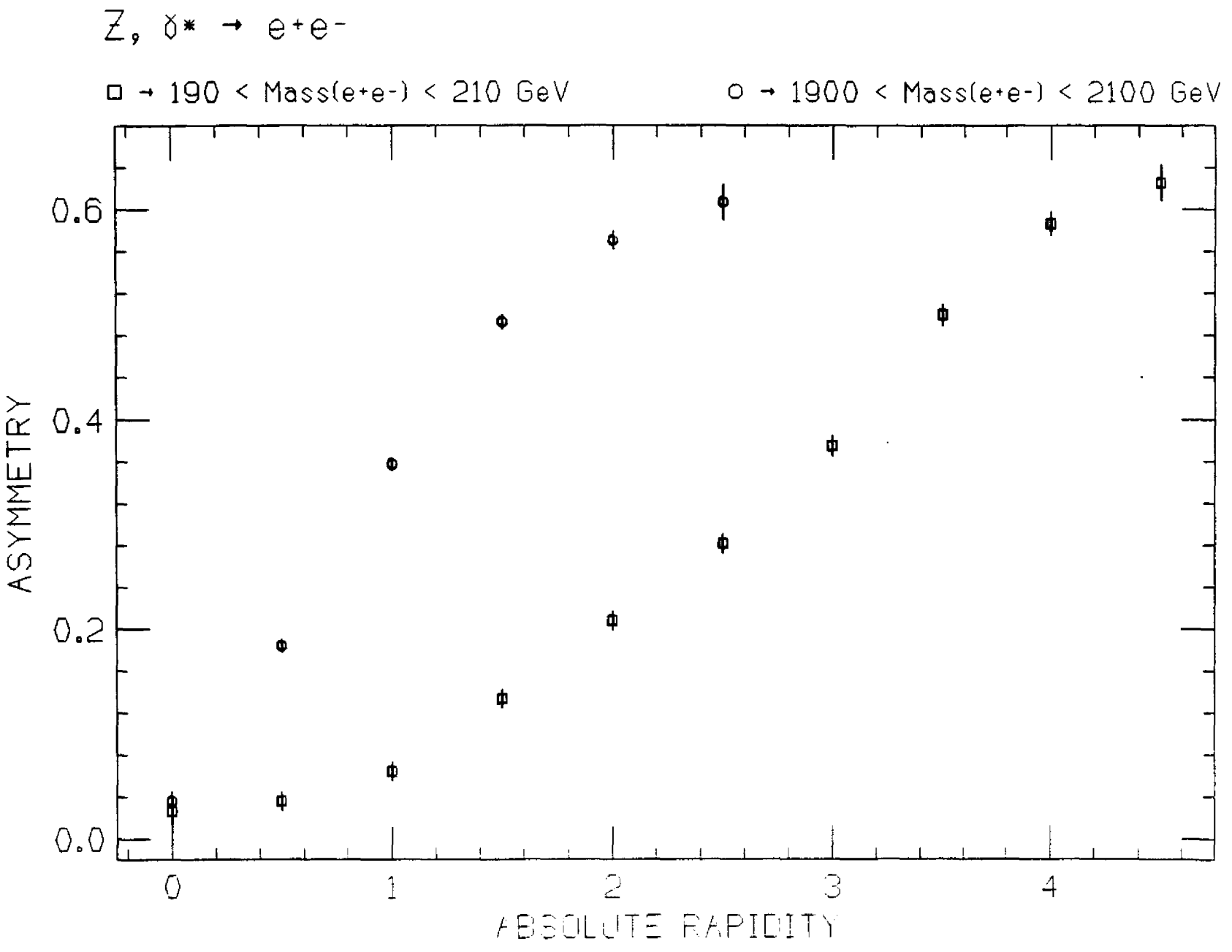
Z, γ* → e+e-
□ → 190 < Mass(e+e-) < 210 GeV
○ → 1900 < Mass(e+e-) < 2100 GeV
ASYMMETRY
0.0
0.2
0.4
0.6
0
1
2
3
4
ABSOLUTE RAPIDITY

Figure 2a

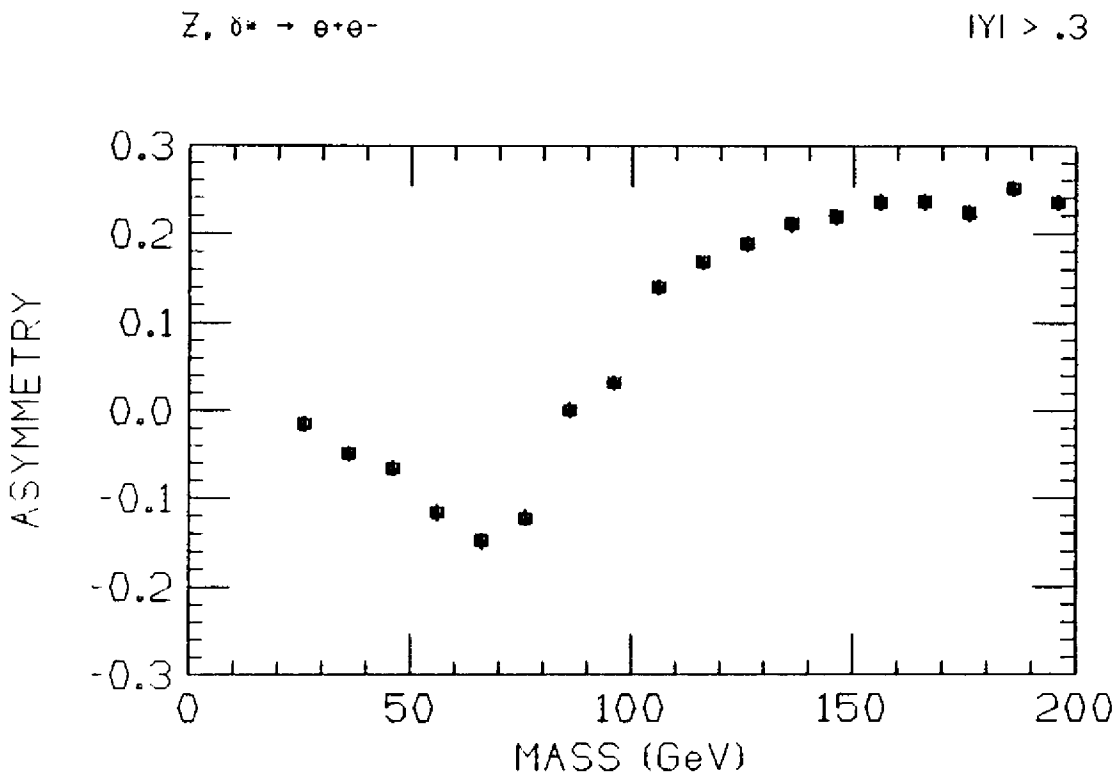

Figure 2b

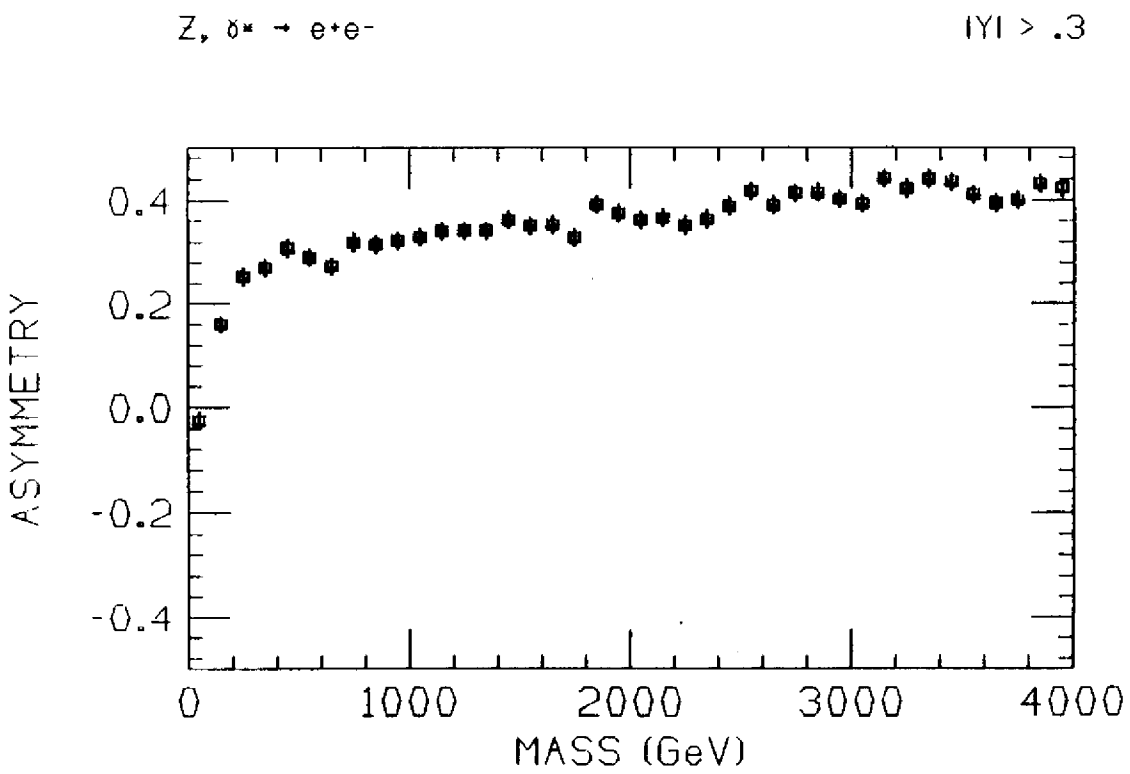

Figure 3

$Z, \gamma^* \rightarrow e^+e^-$

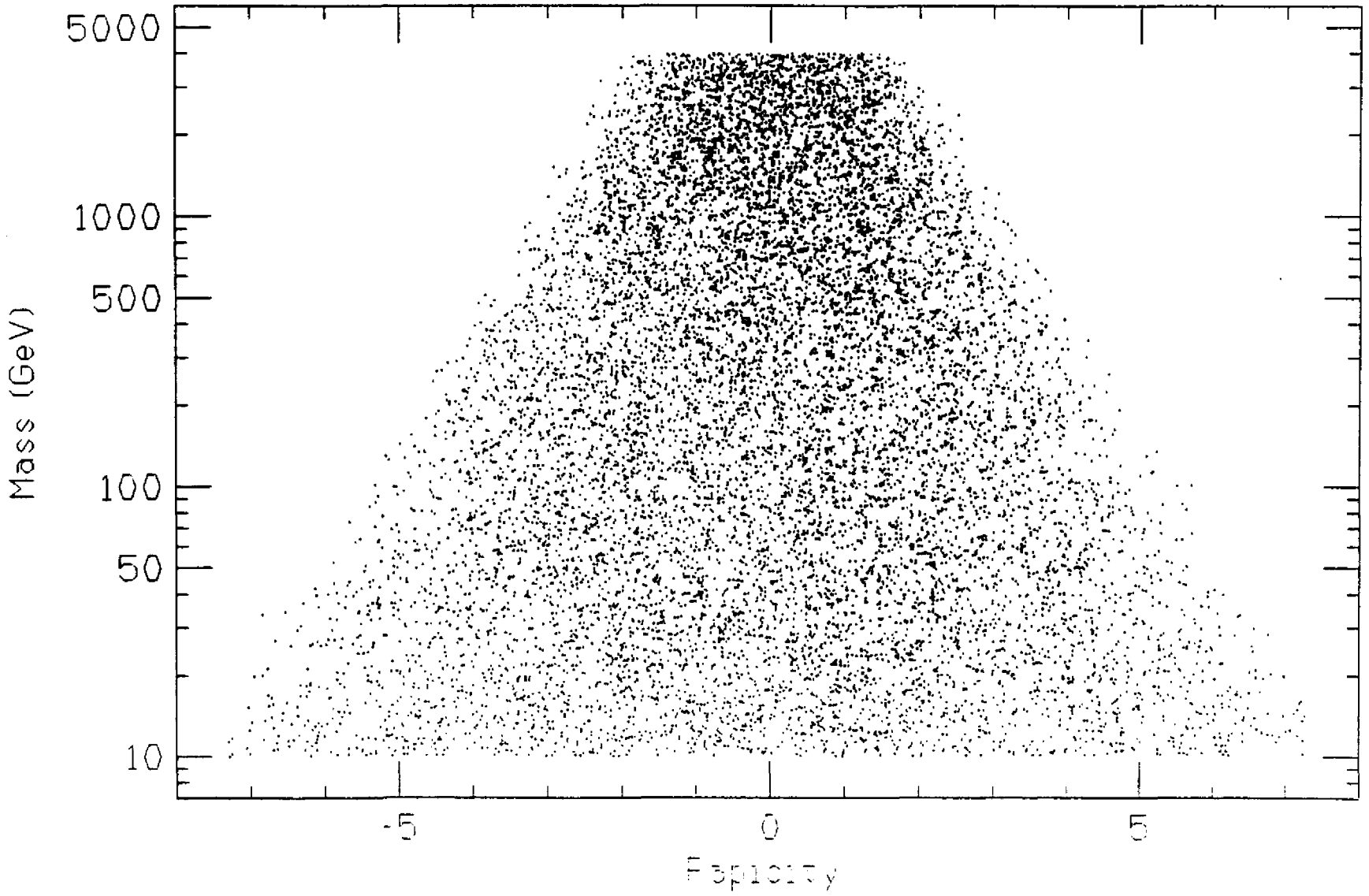

figure 4

Z', Z, $\gamma^* \rightarrow e^+e^-$

Mass(e+e-) = mass Z (lowest curve), 200 GeV, 500 GeV, 1 TeV, 2 TeV, 4TeV

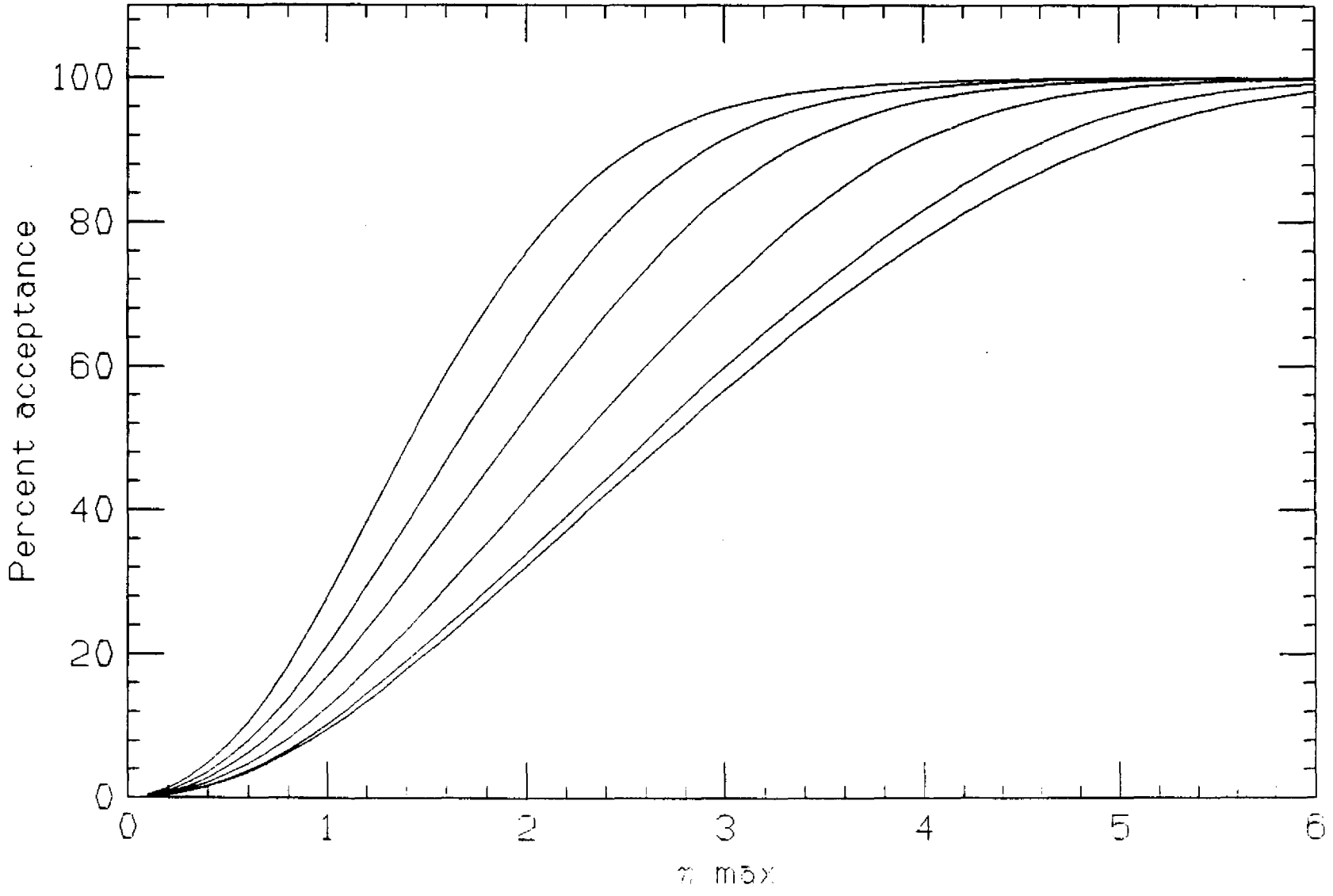

figure 5a

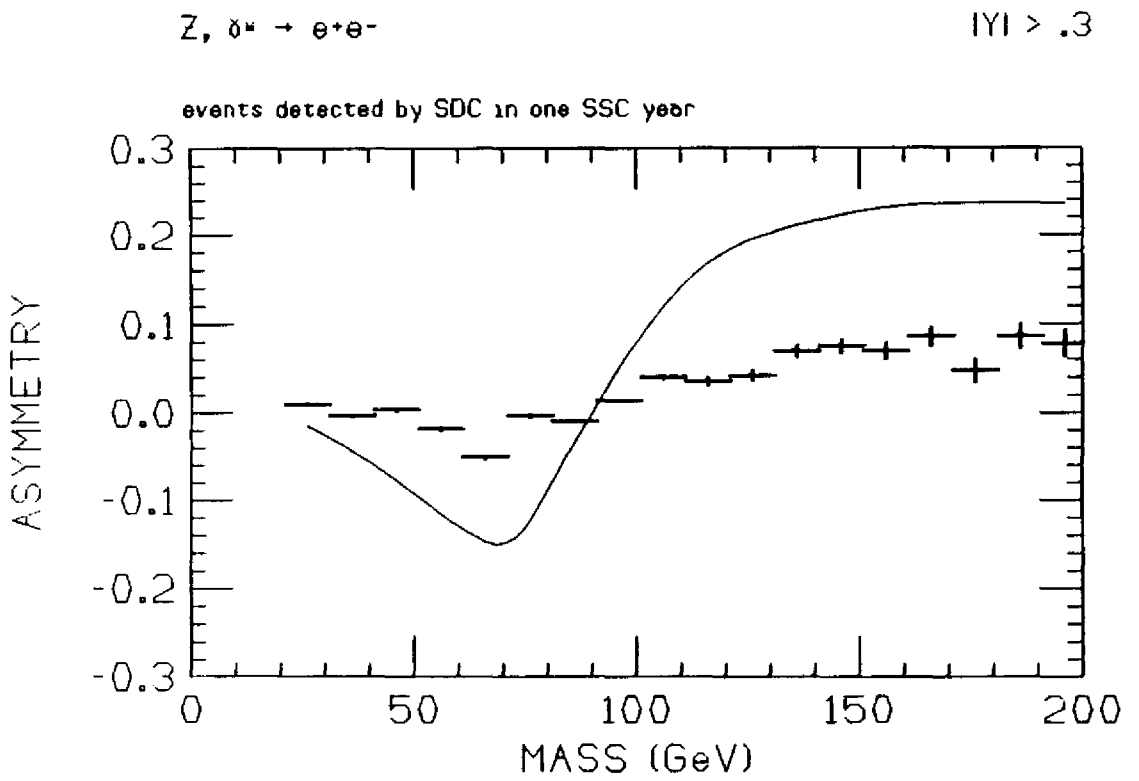

figure 5b

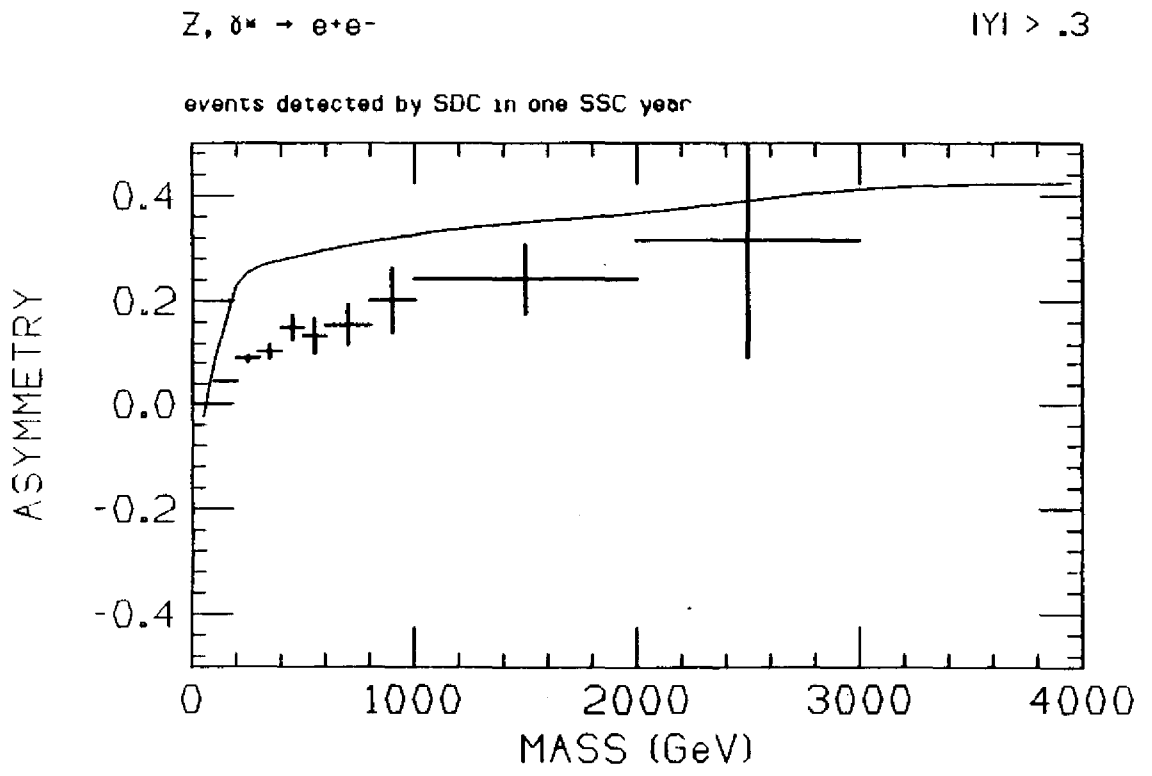

Figure 6

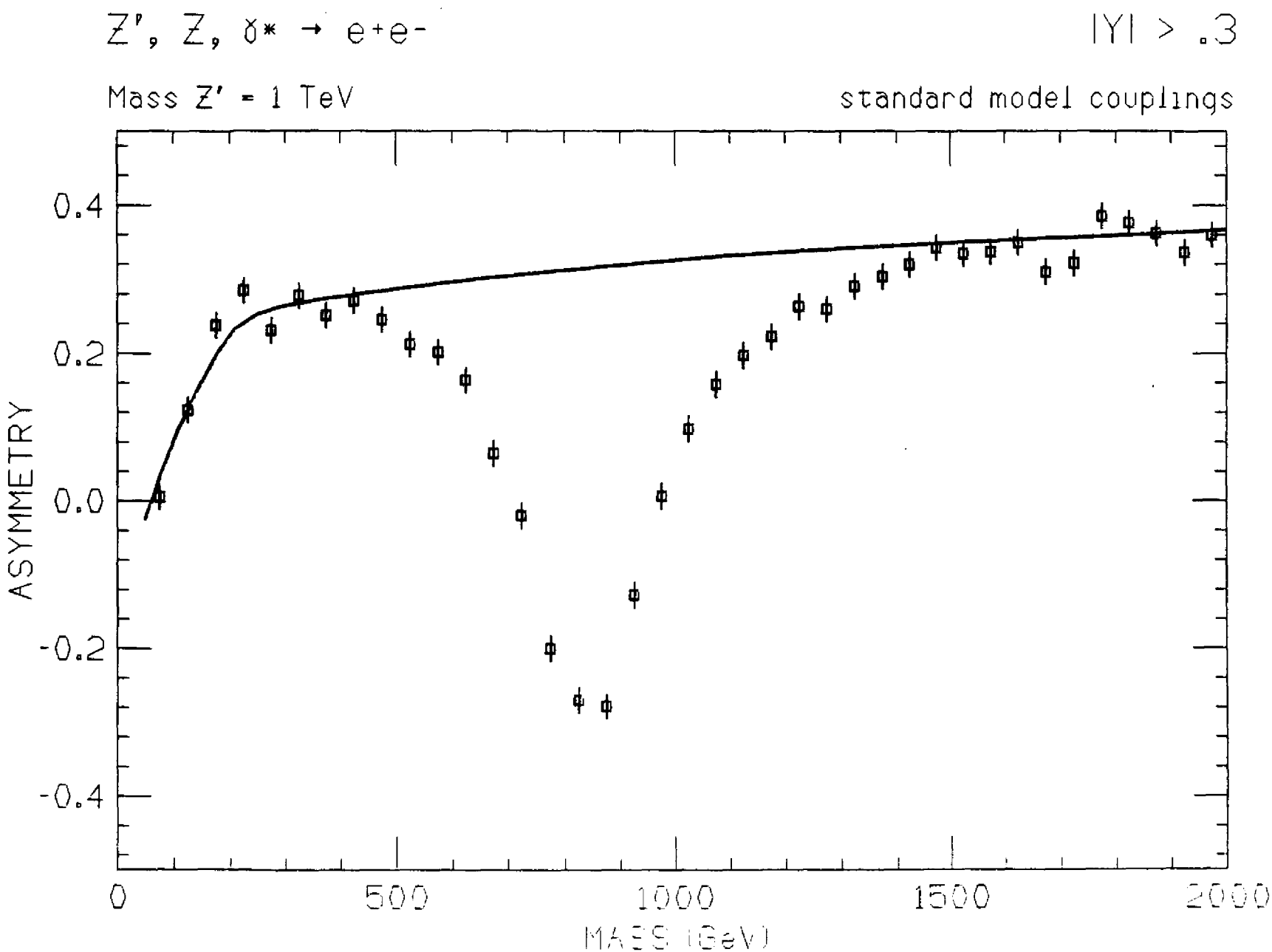
Z', Z, γ* → e+e-
|Y| > .3
Mass Z' = 1 TeV
standard model couplings
ASYMMETRY
0.4
0.2
0.0
-0.2
-0.4
0
500
1000
1500
2000
MASS (GeV)

Figure 7

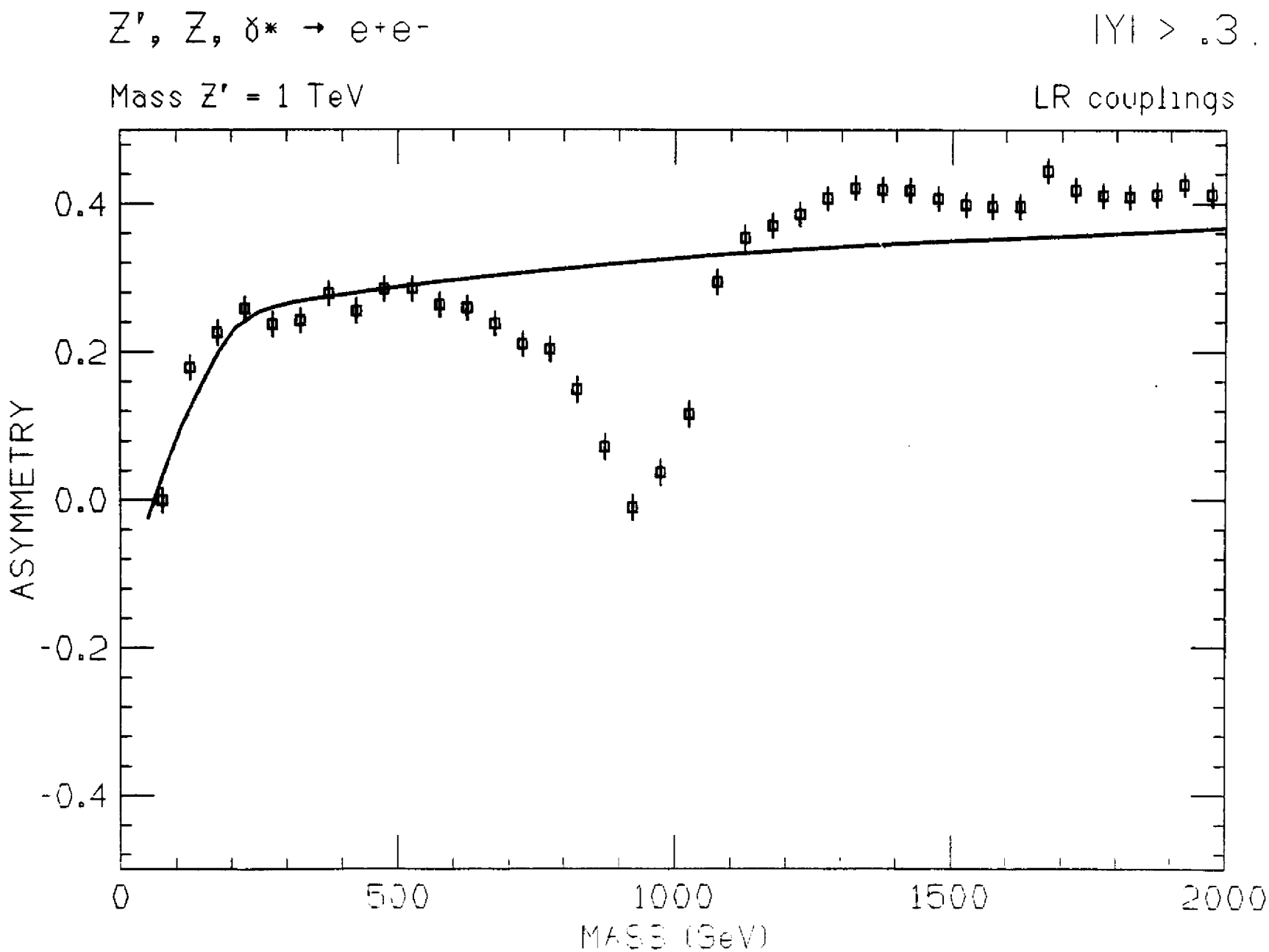
Z', Z, γ* → e+e-
|Y| > .3
Mass Z' = 1 TeV
LR couplings
ASYMMETRY
0.4
0.2
0.0
-0.2
-0.4
0
500
1000
1500
2000
MASS (GeV)

Figure 8

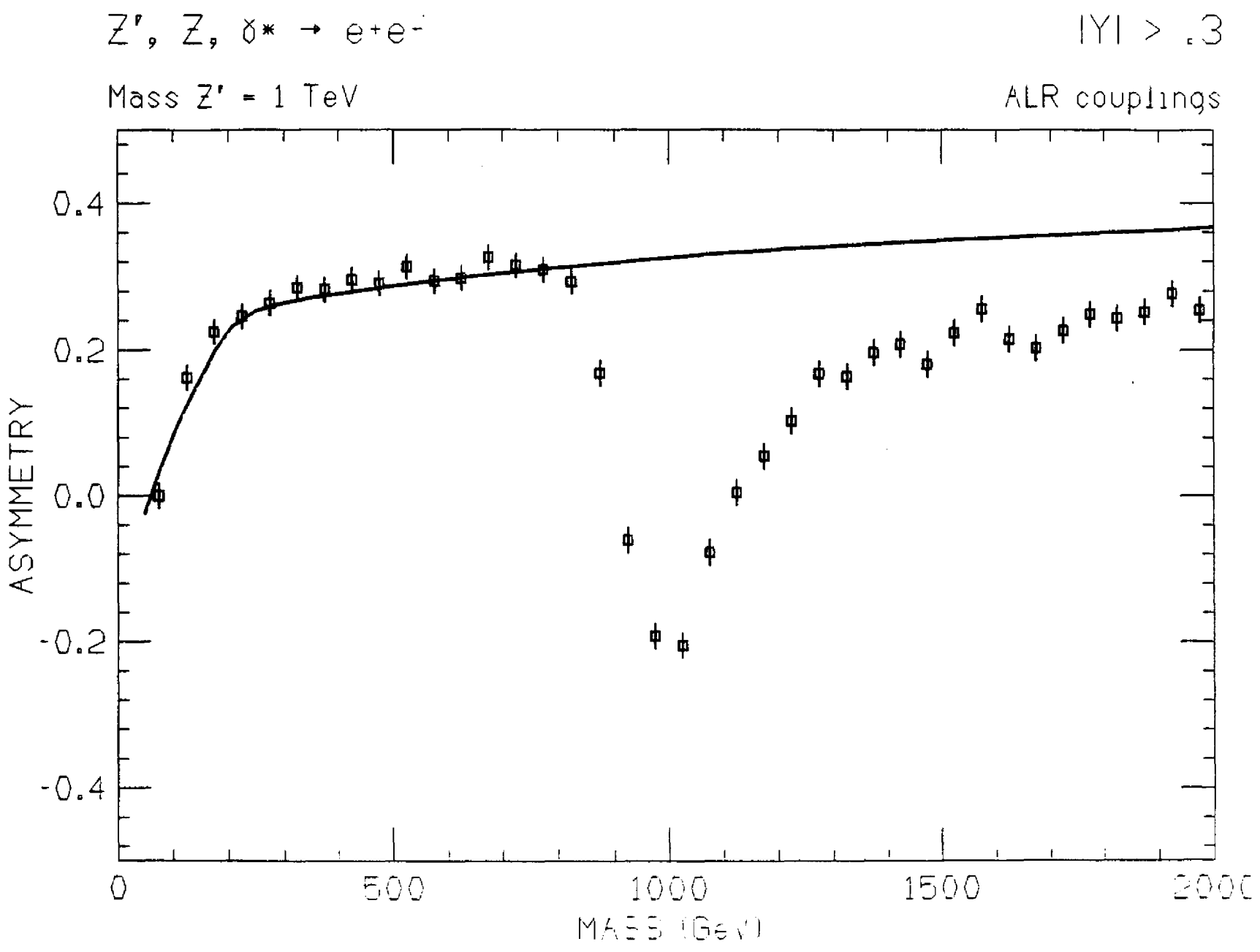
Z', Z, γ* → e+e-
|Y| > .3
Mass Z' = 1 TeV
ALR couplings
ASYMMETRY
0.4
0.2
0.0
-0.2
-0.4
0
500
1000
1500
2000
MASS (GeV)

Figure 9

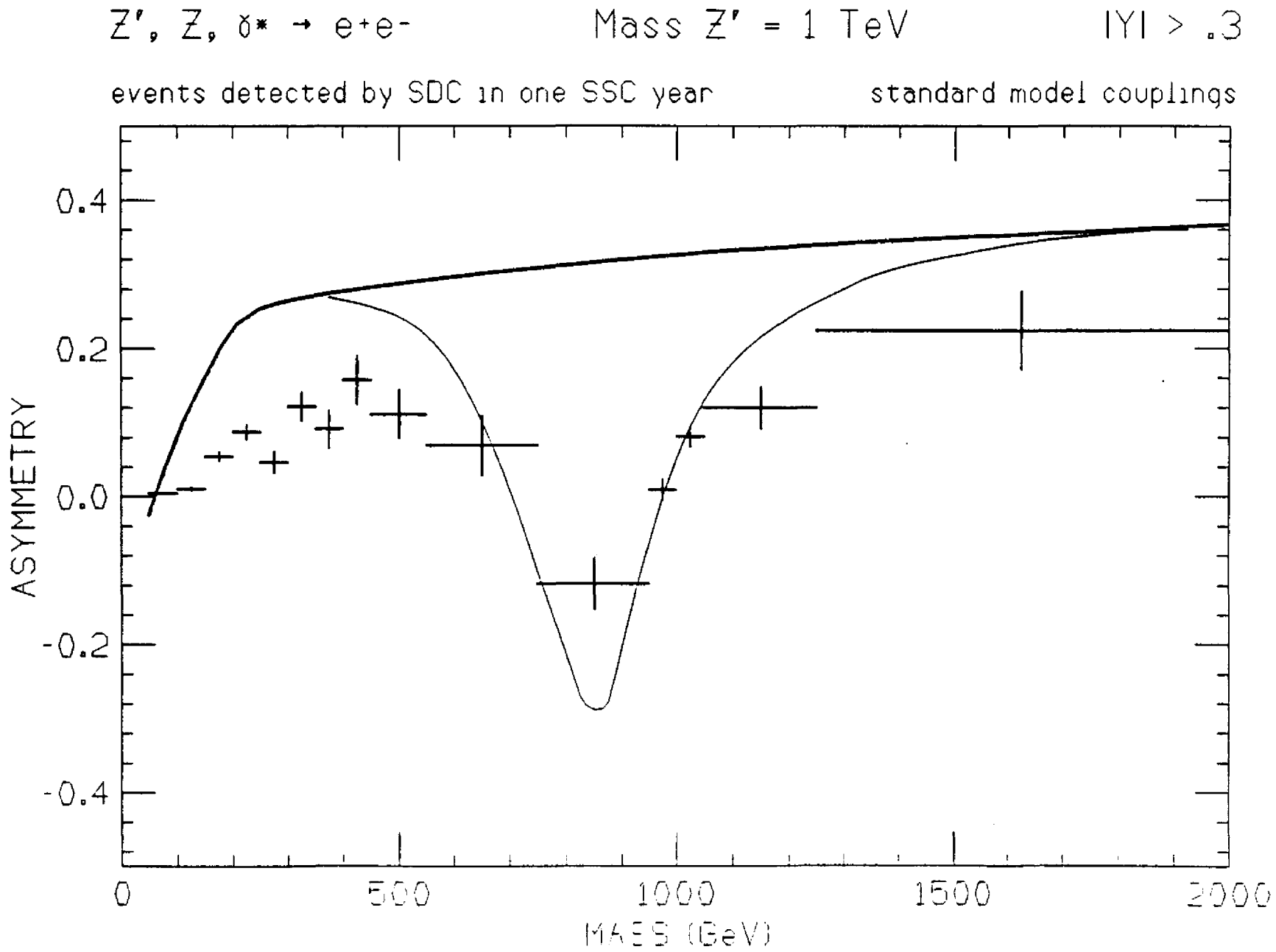
Z′, Z, γ* → e+e-
Mass Z′ = 1 TeV
|Y| > .3
events detected by SDC in one SSC year
standard model couplings
ASYMMETRY
0.4
0.2
0.0
-0.2
-0.4
0
500
1000
1500
2000
MASS (GeV)

Figure 10

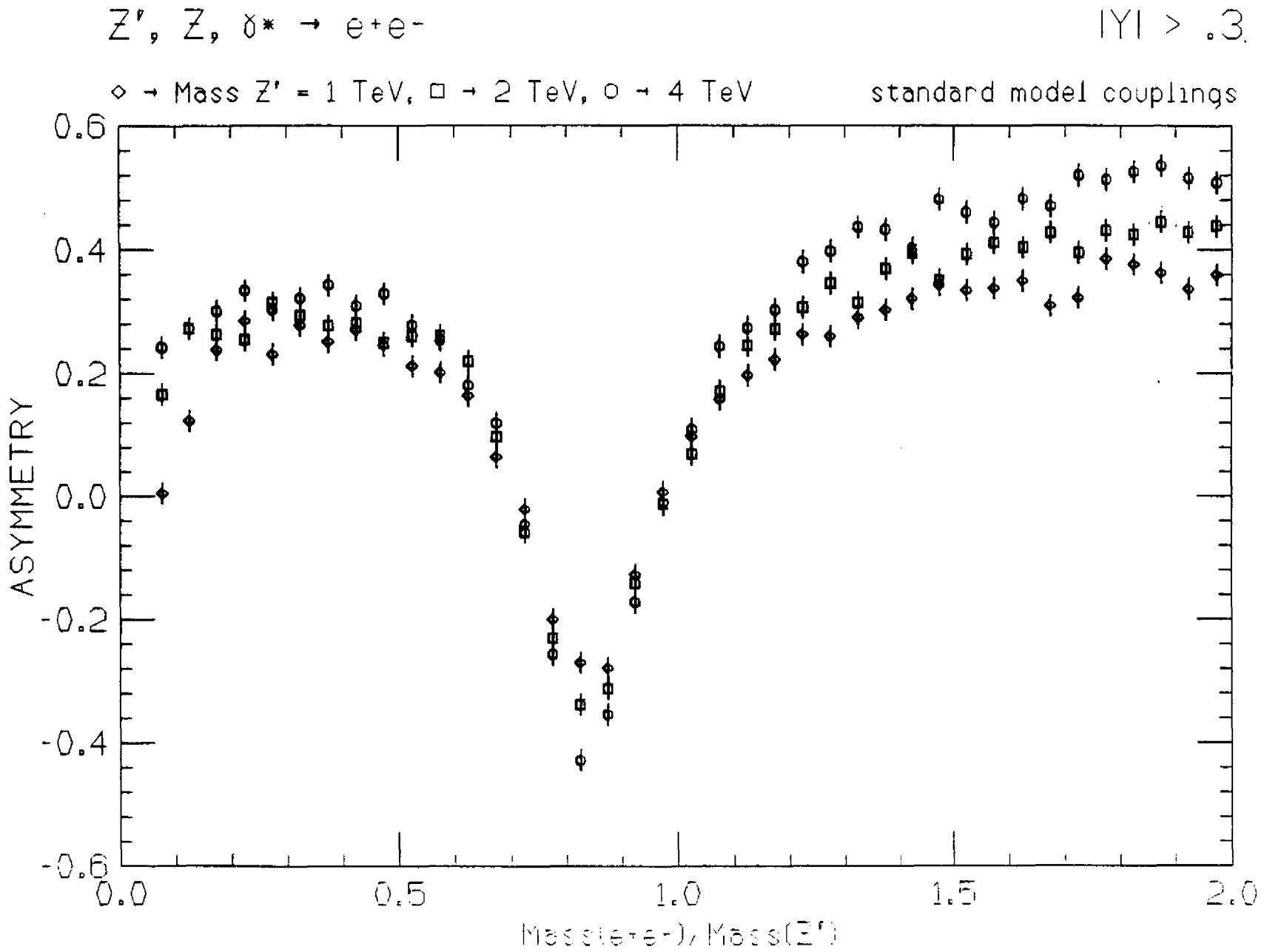
Z', Z, γ* → e+e-
|Y| > .3
◇ → Mass Z' = 1 TeV, □ → 2 TeV, ○ → 4 TeV
standard model couplings
ASYMMETRY
0.6
0.4
0.2
0.0
-0.2
-0.4
-0.6
0.0
0.5
1.0
1.5
2.0
Mass(e+e-)/Mass(Z')